Structure and Mobility in Poly(ethylene oxide)/Poly(methyl methacrylate) Blends Investigated by ^{13}C Solid-State NMR

Staffan Schantz[†]

Department of Polymer Technology, Chalmers University of Technology, S-412 96 Göteborg, Sweden

Received October 18, 1996; Revised Manuscript Received December 26, 1996[⊗]

ABSTRACT: Solid-state ^{13}C CP/MAS/DD NMR measurements have been carried out at 300 K on melt-mixed blends of poly(ethylene oxide)/atactic poly(methyl methacrylate) (PEO/*a*-PMMA) in the concentration range 10/90 to 75/25. Several relaxation times for protons and carbons, i.e. relaxation in the rotating frame ($T_{1\rho}(^1H)$ and $T_{1\rho}(^{13}C)$) and in the laboratory frame ($T_1(^1H)$ and $T_1(^{13}C)$), have been studied. From the carbon relaxations, we conclude that mixing is intimate enough to cause a reduction in local chain mobility for amorphous PEO. Although intermolecular spin diffusion contributes to the proton relaxations in accordance with homogeneity, $T_1(^1H)$ and $T_{1\rho}(^1H)$ data show signs of incomplete averaging. The proton relaxation behavior indicates the existence of heterogeneous domains with shortest dimensions in the nanometer range, which is further supported by the carbon relaxation decays and equilibrium ^{13}C MAS/DD spectra.

Introduction

The increasing interest in polymer blends is mainly due to their importance in the development of new materials with designed properties. Among the various blends of recent attention, poly(ethylene oxide)/poly(methyl methacrylate) (PEO/PMMA) has been extensively investigated. It is generally considered that PEO/PMMA blends are miscible in the liquid state above the melting temperature of PEO ($T_m \sim 338$ K).[1] This is based on numerous experimental and theoretical studies. A single, concentration-dependent glass transition is reported for blends rapidly cooled into the glassy state.[2−4] Investigations of melt dynamics using techniques such as NMR[5−8] and rheometry[9] indicate extensive molecular mixing. Other studies support the view that the blend components maintain distinct relaxation behavior, although different from the pure homopolymer characteristics.[3,10]

A great deal of work has been directed toward the thermodynamics of PEO/PMMA and in particular on the determination of the binary interaction parameter, χ. Small-angle neutron scattering[11,12] (SANS), melting point depression,[13] and pressure−volume−temperature measurements[14,15] give small and negative values of χ in general, consistent with a weakly interacting miscible system. In some of these investigations however temperature and concentration dependences for the interaction parameter have been noted.[2,12] Recent SANS data of PMMA-rich blends (with either of the two polymers deuterated) suggest an upper critical solution temperature at ca. 350 K.[12] Also a lower critical solution temperature has been predicted from theoretical considerations based on the corresponding states theory.[16]

In the solid state phase separation occurs under such conditions that crystallization of PEO can take place, i.e. below the PEO melting temperature and for PEO-rich blends. It is clear that the addition of PMMA influences the crystallization kinetics and lowers the melting point of PEO.[13,17−20] Blends with PMMA contents higher than ∼70−80% are completely amorphous and are reported as being miscible. In fact, it is commonly thought that the melt homogeneity is preserved in the amorphous phase also when crystallization of PEO occurs and that PMMA, completely mixed with amorphous PEO, is incorporated between the crystalline lamellae in the PEO crystals. Data from many techniques support this scenario, for example small-angle X-ray scattering[21,22] (SAXS), SANS,[23] NMR,[8] and microscopy.[2] Some of these studies however suggest that PEO/isotactic PMMA (*i*-PMMA) is an exception and forms separated amorphous phases, the effect depending critically on the molar mass of PMMA.[8,22] There are also a few recent investigations which report on a very local demixing in the disordered phase of solid PEO/atactic PMMA (*a*-PMMA).[23−25] Combined SANS/SAXS measurements suggest the existence of a substantial amorphous interphase on the PEO crystal surface from which PMMA is excluded.[23] For blends stored up to 1 month at room temperature, two glass transitions have been observed.[17] One may conclude that despite all research effort there are conflicting reports regarding the level of mixing for PEO/PMMA, in particular for solid blends.

^{13}C solid-state NMR has proven a very useful method for investigations of local structure and mobility in polymers.[26−29] High-resolution spectra, obtained by the combination of cross polarization (CP) with magic angle sample spinning (MAS) and proton decoupling (DD), not reveal only the primary repeat unit structure but are also sensitive to different conformations. Individual relaxation times obtained from resolved carbon resonances give information on the local mobility; spin−lattice relaxation times in the laboratory reference frame ($T_1(C)$) and in the rotating frame ($T_{1\rho}(C)$) respectively probe motional frequencies in the ∼MHz and ∼kHz region. The CP/MAS/DD experiment provides in addition the possibility to measure proton relaxation times ($T_1(H)$ and $T_{1\rho}(H)$) indirectly via carbon spins and therefore with maintained high resolution.[27] Proton relaxations are sensitive to domain sizes by the process of spin diffusion and can be used to study miscibility in polymer blends.[27−29]

In the present work we have made use of ^{13}C CP/MAS/DD NMR for investigation at 300 K of PEO blends with *a*-PMMA over the concentration range of 10/90 to 75/25 (PEO/*a*-PMMA). The molecular structure has been

[†] Present address: Department of Drug Delivery Research, Pharmaceutical R&D, Astra Hässle AB, S-431 83 Mölndal, Sweden.

[⊗] Abstract published in *Advance ACS Abstracts,* February 1, 1997.

S0024-9297(96)01538-0 CCC: $14.00

studied with focus on the level of intermolecular mixing by ^{13}C spectra and proton relaxation times. The local chain mobility has been investigated with measurements of carbon relaxation times, to our knowledge not previously reported for solid PEO/PMMA blends.

Experimental Section

Materials. The *a*-PMMA used (*6N*, from Röhm GmbH) has molar mass averages $M_n = 47$ kg/mol and $M_w = 90$ kg/mol, respectively. The DSC glass transition temperature (T_g) is 368 K.[30] The stereochemical configuration was investigated by proton NMR of *a*-PMMA/deuteriochloroform solutions at room temperature. Relative concentrations of triads were found to be $rr = 43\%$, $mr = 41\%$, and $mm = 16\%$, where *m* and *r* denote meso and racemic diads, respectively. This polymer contains a small fraction of methyl acrylate (6 mol %, determined by ^{13}C NMR). The PEO, purchased from Scientific Polymer Products, has $T_g = 206$ K and an $M_w = 200$ kg/mol (reported value by the supplier).[30] Before blending, the materials were thoroughly dried under vacuum for at least 24 h. The homopolymers were subject to the same treatment as the blends; see below.

Several PEO/*a*-PMMA blends of compositions ranging from 10/90 to 75/25 (PEO/*a*-PMMA, by weight) were prepared by melt mixing in a Brabender Melt Mixer (PLE 651). The blends were processed at 453 K for 10 min at 40 rpm. After mixing, the samples were allowed to crystallize at room temperature in a dry atmosphere for about 2 months before experiments started. No further crystallization was observed in ^{13}C spectra or in NMR relaxation behavior, within the experimental accuracy, over the time of investigations (14 months).

NMR Methods. High-resolution solid-state NMR experiments were carried out at 75.4 and 299.9 MHz for ^{13}C and ^{1}H, respectively, using a Varian VXR300 spectrometer. The instrument is equipped with a high-power amplifier for proton decoupling and a Varian CP/MAS/DD (cross polarization/magic angle spinning/dipolar decoupling) probe. Spectra were externally referenced to the aromatic carbon signal of hexamethylbenzene (132.2 ppm). Samples were packed as powders in silicon nitride rotors with Torlon endcaps (Torlon is a poly(amide−imide) copolymer and gives a very weak ^{13}C background which however does not interfere with the results presented in this article). The MAS frequency was set to 5.1 kHz and the sample temperature was 300 ± 3 K in most of the experiments. Cross polarization was performed at 36 kHz (7 μs $\pi/2$ pulses for ^{13}C and ^{1}H), the proton decoupling strength was approximately 70 kHz, and the delay between succesive acquisitions was 3 s. Direct polarization ^{13}C MAS/DD NMR spectra were obtained following single $\pi/2$ pulses and with a recycle delay of 75 s.

Rotating and laboratory frame spin−lattice relaxation times for both protons and carbons were obtained within the standard cross polarization scheme. For proton relaxations we used either a spin-lock sequence with varied duration (for $T_{1\rho}(H)$)[27] or an inversion−recovery sequence (for $T_1(H)$)[31] respectively followed by cross polarization and detection through the carbons. Carbon $T_{1\rho}(C)$ was determined by varying the carbon spin-lock time without proton irradiation after cross polarization.[26] $T_1(C)$ was obtained using the CP-T_1 method as described by Torchia.[32] In the relaxation measurements the contact time was generally set to 100 μs and the recycle delay time was chosen in the range 3−10 s, depending on the relaxation behavior of the sample investigated and on the type of experiment. For each spectrum in the arrayed experiments, 1000−5000 fid's were accumulated, repeatedly cycling through the different time values.

Results and Discussion

^{13}C NMR Spectra. In Figure 1 are shown ^{13}C CP/MAS/DD spectra of PEO, *a*-PMMA, and some of their blends at 300 K. Pronounced changes occur for the PEO resonance as the composition of the blends is varied. For blends with PEO concentrations in the range 10−28%, the full width at half-height is about 130 Hz,

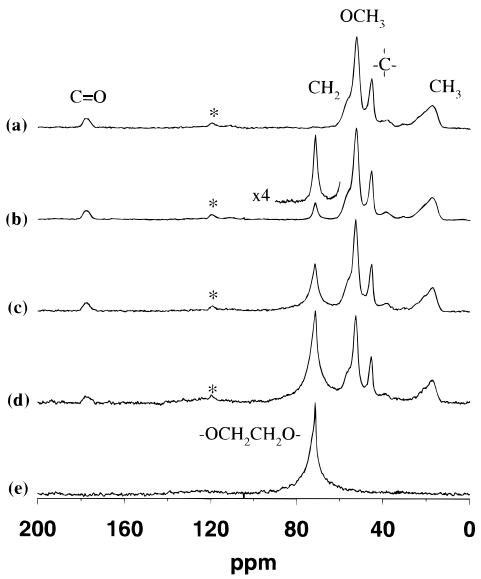

Figure 1. ^{13}C CP/MAS/DD spectra at 300 K of PEO/PMMA: (a) 0/100, (b) 10/90, (c) 50/50, (d) 75/25, and (e) 100/0. The use of a short CP-time (100 μs) reveals major changes in the PEO lineshape at ~71 ppm. Spinning sidebands are marked with an asterisk (MAS frequency = 5.1 kHz).

whereas for higher concentrations the peak broadens significantly to several hundred Hz. For the latter PEO-rich blends the asymmetric lineshape suggests that the PEO resonance is composed of at least two components; see Figure 1. It is well known that the PEO spectrum at room temperature shows a resonance containing slightly shifted (~1 ppm) narrow and broad components respectively due to the presence of both amorphous and crystalline regions.[33−35] The crystalline peak at ~72 ppm reflects a helical structure with a period of seven units in two turns with trans (COCC)−gauche (OCCO)−trans (CCOC) for the repeat unit, $-CH_2CH_2O-$.[36] In the amorphous phase the random conformational structure results in a resonance at ~71 ppm. The large difference in linewidth between the two components is mainly due to differences in mobility. At room temperature the amorphous phase in pure PEO is well above the glass transition temperature (T_g for PEO used in the present study is 206 K), which results in a relatively narrow resonance due to the motionally averaged $^{13}C-^{1}H$ dipolar interaction. The crystalline component is homogeneously broadened; i.e. it reflects the interference between molecular motions and the proton decoupling field (DD).[33,35] Note that the CP/MAS/DD spectra in Figure 1 are not quantitative due to the short CP time needed to acquire the crystalline PEO component.

From the above discussion it is clear that the changes of the PEO resonance in Figure 1 are mainly due to the appearance of a crystalline phase for blends with PEO concentrations higher than ~30%. In order to quantify the degree of crystallinity, we performed a ^{13}C MAS/DD experiment with a long recycle delay (75 s) for correct spin counting. The PEO lineshape is well fitted to a sum of two Lorentzians (crystalline and amorphous components respetively at 72.1 ± 0.5 and 71.3 ± 0.3 ppm) for blends with a PEO content higher than 28%; see Figure 2 (in some of the deconvolutions, a constraint was used: the width of the amorphous peak was held fixed to the value obtained for long $T_{1\rho}$ relaxation delays; see next section). Below this limit, a single Lorentzian (amorphous component at 71.3 ppm) is sufficient to describe the lineshape. A two-peak band analysis for semicrystalline PEO has been reported to describe also

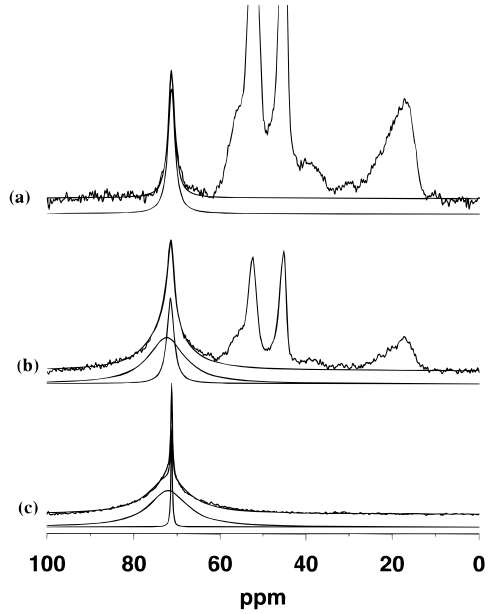

Figure 2. ^{13}C MAS/DD spectra at 300 K (recycle pulse delay = 75 s) of PEO/PMMA: (a) 10/90, (b) 50/50, and (c) 100/0. The PEO lineshape is fitted to a sum of two Lorentzians ((b) and (c)) or to a single Lorentzian ((a)).

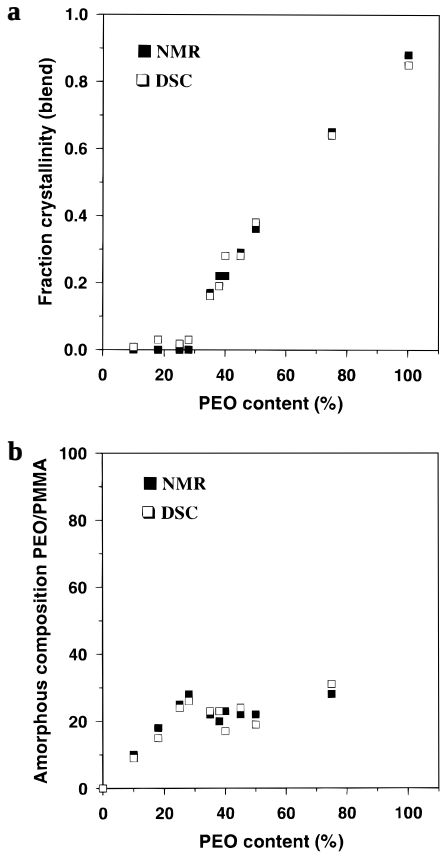

Figure 3. Fraction of crystallinity (a) and amorphous phase composition (b) for PEO/PMMA blends as a function of PEO content. DSC data (□) are from Ref. 37. NMR data (■) are obtained from a two-component analysis of ^{13}C MAS/DD equilibrium lineshapes (see Figure 2).

the proton NMR lineshape quite well.[35] Results of the calculated crystalline fractions in the blends are presented in Figure 3a. For comparison, DSC data from ref 37 for blends with the same thermal history are included in the figure (the degree of crystallinity was calculated in ref 37 by taking 203 J/g as the enthalpy

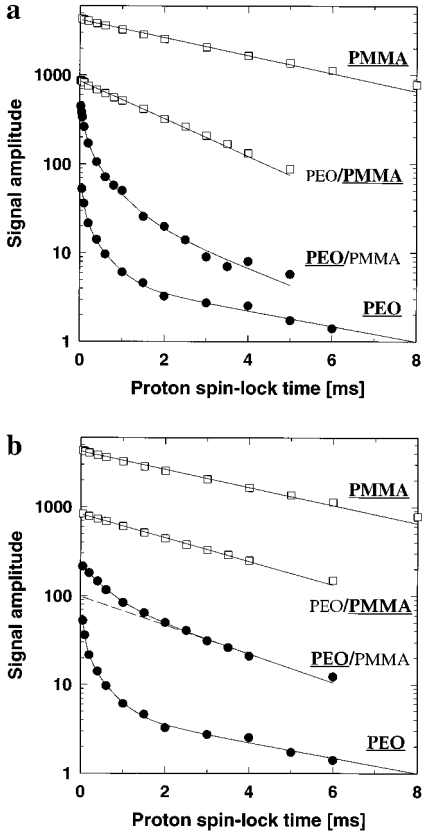

Figure 4. Proton $T_{1\rho}$(H) relaxation behavior at 300 K for PEO/PMMA: (a) 75/25, and (b) 10/90. Data for the homopolymers are included in (a) and (b). The solid lines are exponential or multi-exponential fits to the data.

of fusion for 100% crystalline PEO). The two methods are in excellent agreement and show a gradually increasing crystalline fraction with increasing PEO content above ~30%; see Figure 3a. From the quantitative analysis it is possible to correct and determine the real composition of the amorphous phase in the blends; see Figure 3b. Interestingly, the amorphous PEO content changes little in the semicrystalline blends and does not exceed 30% even for the PEO-rich blends. The results of morphological changes are in line with the general finding for PEO/*a*-PMMA of a significantly depressed crystallization for PEO due to the presence of noncrystallizable PMMA.[17−20]

Besides the changes in relative intensities of the two PEO resonances in the blends related to the changes in morphology, the widths are affected by blending. This is most striking for the amorphous PEO component; the full width at half-height was found to be ~130 Hz in the blends (with a weak concentration dependence) compared to only ~30 Hz for the amorphous component in pure PEO; see Figure 2. The origin of the spectral broadening may well be a reduction in chain mobility for amorphous PEO caused by mixing with less mobile PMMA segments. It has recently been shown that the MAS/DD linewidth is a sensitive probe of mid-kilohertz molecular motions in salt-complexed amorphous PEO.[38] Another contribution to the line broadening may of course be a wider distribution of local environments in the blends giving rise to an inhomogeneous broadening.

Proton Relaxations. More detailed information about the structure of PEO/*a*-PMMA blends is obtained from the proton relaxation behavior. The $T_{1\rho}$(H) decay for PEO is nonexponential over the whole concentration range; see Figure 4 and Table 1. As established in

Table 1. Proton $T_{1\rho}$(H)[a] Values (ms) for PEO, PMMA, and Their Blends at 300 K

PEO/PMMA	PEO			PMMA[b]
0/100				4.3
10/90		0.6 (65%)	3.3 (35%)	3.4
18/82		0.6 (79%)	2.5 (21%)	2.4
38/62	0.1 (30%)	0.4 (53%)	2.2 (17%)	2.2
50/50	0.1 (46%)	0.4 (40%)	2.4 (14%)	2.4
75/25	0.1 (63%)	0.4 (30%)	2.3 (7%)	2.1
100/0	0.1 (68%)	0.4 (26%)	5.0 (6%)	-

[a] Estimated accuracy: for decays fitted to single exponentials ±5%; for multiexponentials ±20%. [b] Average for the protons of PMMA.

earlier studies of PEO, the fast initial magnetization decay (time constant 0.1 ms) corresponds to the broad crystalline component and the long time decay (5 ms in pure PEO) is due to the relaxation of the narrow peak from amorphous regions.[34,35] The relative amplitudes of the amorphous/crystalline relaxation components (Table 1) change with composition qualitatively in accordance with the lineshape and DSC data;[37] see Figure 3 and Table 1. Clearly, the crystalline relaxation decay is absent for the PMMA-rich blends with PEO contents below ~30%. For the semicrystalline blends the strongly nonexponential PEO relaxation is, in fact, best fitted to a sum of three exponential terms (Table 1). The intermediate $T_{1\rho}$(H) component of 0.4−0.6 ms appears to be present also for the amorphous blends and cannot from our measurements be related to a unique third phase with respect to a distinctly different mobility (see next section) or spectral feature (see previous section). Instead, we suggest that it reflects the influence of spin diffusion on the amorphous relaxations. Spin diffusion is the spatial transport of magnetization among protons, which is mediated by dipolar interactions between neighboring spins.[39] The process acts as an averaging mechanism for the relaxations in a blend provided miscibility or if the domain sizes are of a few nanometers dimension only.[27]

In all blends investigated the $T_{1\rho}$(H) relaxations for PEO and PMMA approach a close value for longer spin-lock times. This averaged $T_{1\rho}$(H) of ~2−3 ms is concentration dependent and different from the relaxation times of respective homopolymer (Table 1), which indicates that spin diffusion between PEO and PMMA in well-mixed amorphous regions contributes to the relaxations. In contrast, the time constant for the crystalline PEO relaxation is not sensitive to blend composition due to the phase-separated crystalline regions. To a first approximation, these observations indicate that semicrystalline PEO/*a*-PMMA indeed can be described as a two-phase system: an amorphous phase where PMMA molecules are intimitely mixed with amorphous PEO and a pure crystalline PEO phase.

However, it is interesting to note that the $T_{1\rho}$(H) decay for PEO is biexponential for the amorphous blends with PEO concentrations below ~30%; see Figure 4b and Table 1. Although clearly affected by spin diffusion to PMMA, the relaxations are not completely averaged. In fact, by increasing the CP contact time from 0.1 to 1 ms in the experiments, thereby suppressing the crystalline component due to its rapid relaxation, all the blends show similar two-component PEO relaxations. The results indicate that the amorphous phase is not completely homogeneous in any of the blends investigated. For a molecularly miscible amorphous PEO/PMMA phase we would expect completely averaged single-exponential relaxations, in particular since the amorphous relaxation rates for the homopolymers are relatively close (Table 1). These heterogeneities need not be more than poorly dispersed regions with dimensions of a few nanometers (see below for an estimation of length scales). It is possible that the faster amorphous PEO relaxation (time constant 0.4−0.6 ms) is due to such domains of amorphous nonmixed PEO and that the slower averaged $T_{1\rho}$(H) component originates from completely miscible regions. However, there is not necessarily a one-to-one correspondence between the number of proton relaxation components and the number of physically distinct regions.[40] Amorphous PEO molecules could have a similar nanoheterogeneous environment with a proton relaxation which is not completely averaged by the proximity to PMMA. The latter explanation is supported by the carbon relaxation behavior (see next section) and also by xenon NMR-probe measurements recently performed in our laboratory.[41]

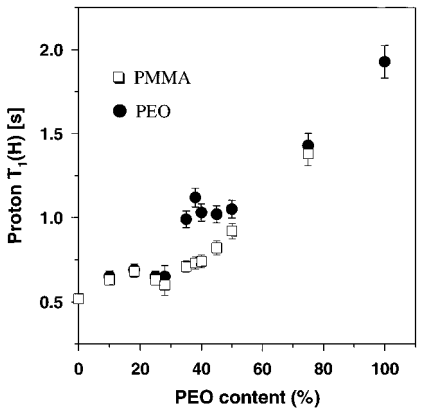

Figure 5. Proton T_1(H) relaxation times at 300 K for PEO/PMMA vs. PEO content.

Results from proton laboratory frame relaxation times, T_1(H), are plotted vs blend composition in Figure 5. Contrary to the $T_{1\rho}$(H) data, all T_1(H)'s were found to be single-exponential processes and for most blends the relaxations are completely averaged by spin diffusion. The two relaxation experiments allow us to estimate roughly the sizes of blend heterogeneities. For complete averaging over the time of relaxation (t) with an effective spin diffusion coefficient (D) the upper limit (l) for a domain is approximately $\langle|l|\rangle = (6Dt)^{1/2}$ (spin diffusion in different geometries results in small changes only of the prefactor in this expression).[42−44] Taking $D = 4.1 \times 10^{-16}$ m^2/s as an average from literature data of PEO[43] and PMMA−PS block copolymers[44] and for $t = T_1$(H) ~ 1.2 s we obtain $\langle|l|\rangle \sim 50$ nm. Similarly, taking into account that for spin diffusion in the rotating frame D is scaled by a factor of $^1/_2$,[44] the $T_{1\rho}$(H) experiment sets the lower limit with $\langle|l|\rangle \sim 2$ nm. Thus the approximate domain sizes are between 2 and 50 nm. This is valid for the amorphous blends with PEO/*a*-PMMA compositions below 30/70 and for the PEO-rich materials, i.e. 75/25 and 100/0 (PEO/*a*-PMMA). For the latter systems the NMR estimate of the domain size seems to agree well with SANS/SAXS data in the same concentration range (although obtained from samples with other thermal histories); values of the long period (interlamellae spacing) are reported to be in the range ~20−50 nm.[21−23] It is then a surprising finding that the T_1(H)'s in the intermediate concentration region of 30−50% PEO in the present study are not completely averaged (Figure 5). This result could be related to the changing distribution and dimension of crystallites in

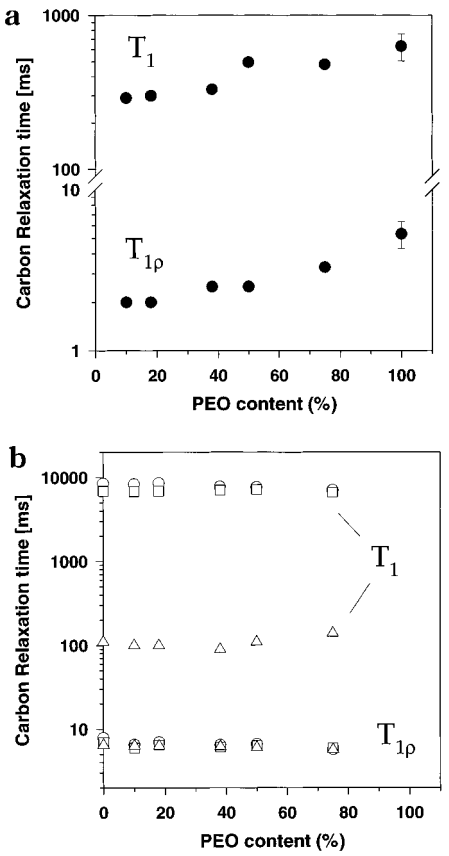

Figure 6. Carbon $T_{1\rho}$(C) and T_1(C) relaxation times at 300 K for PEO/PMMA as a function of PEO content. Results for amorphous PEO (●) are shown in (a) and for PMMA in (b): $-OCH_3$ (○), quaternary carbon (□), and α-CH_3 (△).

Table 2. Carbon Relaxations: T_1(C) and $T_{1\rho}$(C) for PEO in Blends with PMMA at 300 K

	PEO[a]				
PEO/PMMA	$T_{1\rho}$(C) (ms)			T_1(C) (s)	
10/90			2.0	0.3	
18/82			2.0	0.3	
38/62		0.4 (52%)	2.5 (48%)	0.3 (50%)	15 (50%)
50/50		0.4 (74%)	2.5 (26%)	0.5 (51%)	15 (49%)
75/25	0.1 (52%)	0.8 (41%)	3.3 (7%)	0.5 (40%)	15 (60%)
100/0	0.1 (74%)	0.6 (19%)	5.3 (7%)	0.6 (42%)	15 (58%)

[a] Estimated accuracy: for decays fitted to single exponentials ±5%; for multiexponentials ±20%.

the semicrystalline blends as the composition is varied.[44] The long period from small-angle scattering in the PEO-rich region (above ∼50% PEO) is reported to be very sensitive to the blend composition and may well, if extrapolated, exceed the critical NMR distance (∼50 nm) for blends in the intermediate region.[21−23] Another possible origin for the incomplete averaging in this concentration range could be an amorphous phase separation on a length scale larger than ∼50 nm. Blends in this region are difficult to investigate with standard DSC because the glass transition is masked by the melting transition of PEO.[17] Direct spin diffusion experiments combined with simulations would be helpful for a conclusive explanation of the unusual T_1(H) behavior.

Carbon Relaxations. Results of carbon relaxation are presented in Figure 6 and Table 2. The dramatic changes observed for the PEO relaxations in the various blends are attributed to, on one hand, a varying morphology and, on the other hand, a changed mobility for amorphous PEO. The phase separation due to the the appearance of a crystalline PEO phase for concentrations above ∼30% PEO contents is reflected also in the nonexponential carbon relaxation decays; the crystalline relaxation corresponds to a faster deay in $T_{1\rho}$(C) (0.1−0.4 ms) and a slower component (15 s) in T_1(C) compared to the respective amorphous decays (Table 2). The assignment is based on the continuous changes in the PEO lineshape/chemical shift, as for proton $T_{1\rho}$(H), and is in agreement with earlier reports of PEO.[34] The semicrystalline blends thus show two-component decays in $T_{1\rho}$(C) and T_1(C), respectively. An exception was found for some of the $T_{1\rho}$(C) relaxations (pure PEO and the 75/25 PEO/*a*-PMMA blend; see Table 2), which are best fitted to triple-exponential decays. However, the possible contribution of spin−spin processes to the crystalline PEO relaxation in the latter cases prevents us from a deeper quantitative analysis of these decays[26] (spin−spin contributions are not influencing the amorphous $T_{1\rho}$(C) relaxation as shown in ref 38). The laboratory frame relaxation (T_1(C)) is not complicated by spin−spin relaxation so, in principle, the relative amplitudes of crystalline/amorphous decays should agree with the equilibrium lineshape data in Figure 3. For such an analysis, which is beyond the scope of the present study, one has to correct for the widely different cross polarization behaviors of crystalline/amorphous PEO.[34] Interestingly, the PEO relaxations for the amorphous blends are single-exponential within experimental accuracy, which supports the interpretation of the biexponential proton $T_{1\rho}$(H)'s as being caused by spin diffusion and not by two amorphous PEO populations with different mobilities.

We conclude that the concentration behaviors of the carbon relaxations are in qualitative agreement with the proton relaxations and also with the ^{13}C MAS/DD lineshape data and DSC;[37] see Figures 3−5 and Tables 1 and 2. These results altogether can be explained without invoking a third phase, namely an amorphous PEO interphase connecting amorphous PEO/*a*-PMMA with PEO crystals. Perhaps the concentration of the interphase is too low for detection in unenriched samples by ^{13}C NMR. Another possibility is that the mobility at the interphase is close to that of the crystalline or amorphous phase and cannot be resolved in our relaxation time experiments.

We also note that recent IR studies indicate the presence of two PEO polymorphs in semicrystalline blends with PMMA.[17,45,46] The present results do not reveal a second PEO crystal structure as judged by the ^{13}C lineshapes or the T_1(C) decays in which the crystalline time constant was found to be constant with blend composition (Table 2).

Next we turn to the dynamics of the amorphous phase in the blends. Time constants for the amorphous PEO relaxations are plotted in Figure 6a (see also Table 2) and for the carbons of *a*-PMMA in Figure 6b (the carbonyl carbon relaxation is not included due to its low intensity for the CP time chosen). For amorphous PEO at room temperature both $T_{1\rho}$(C) and T_1(C) are on the high temperature side of their respective minimum.[38,47] Consequently, the addition of PMMA clearly causes a reduction in segmental mobility for PEO, as shown by the gradually decreasing relaxation time values for increasing PMMA concentration; see Figure 6a and Table 2. The largest changes compared to pure PEO are found for the amorphous blends as expected with a ∼50% reduction at most; from 5.3 ms and 0.6 s in pure

PEO to 2.0 ms and 0.3 s in the blends (10/90 and 18/82 PEO/*a*-PMMA) respectively for $T_{1\rho}$(C) and T_1(C) (Figure 6a and Table 2). It is notable that the changes in T_1(C) are of the same order as those reported from measurements of molten PEO/PMMA at higher temperatures.[7]

Analogous to our finding of a lowered PEO mobility in the blends, it is likely that *a*-PMMA segments move faster and/or with larger amplitude by the presence of amorphous PEO molecules. The *a*-PMMA carbon relaxations are however unaffected by blend composition; see Figure 6b.[48] This can be understood by considering the molecular motions responsible for the relaxations. In PMMA at around room temperature the α-CH_3 group reorientations are much decoupled from the extremely slow segmental motions below T_g.[49,50] Hence, the protons of the methyl group can move in the glassy state with part of the correlation time distribution even in the megahertz region and relax the neighboring carbons in the monomer unit despite the r^{-6} proton−carbon distance dependence of relaxation rates. Consequently, small changes in segmental mobility of *a*-PMMA caused by the addition of PEO may not be probed in the T_1(C) experiment at room temperature (Figure 6b). Similar findings of plasticized PMMA have been reported by Edzes and Veeman.[50] An α-CH_3-dominated relaxation may explain also the rotating frame relaxation results; see Figure 6b. In addition, nonmotional spin−spin processes may contribute to the latter relaxation, which would furthermore decrease the sensitivity to changes in motion.[49] We do not expect however large changes in mobility for *a*-PMMA in the light of the results presented in Figure 3b; the amount of mobile amorphous PEO does not exceed ∼30% even in the 75/25 (PEO/*a*-PMMA) blend with the highest amount of PEO.

In the case of amorphous PEO above T_g, both $T_{1\rho}$(C) and T_1(C) relaxations have been shown to be caused by segmental motions which are linked to the glass transition.[38,47] By comparing the present relaxation data with published temperature-dependent carbon relaxations in PEO[47] and PEO−salt complexes,[38] we estimate the average correlation time curve ($\langle\tau\rangle$ vs temperature) to shift to higher temperatures by ∼15 K, from pure PEO to the completely amorphous blends (10/90 to 18/82 PEO/*a*-PMMA). Using the free volume dependence of $\langle\tau\rangle$ reported by Dekmezian et al. for PEO,[47] this corresponds to a rather modest increase at 300 K from $\langle\tau\rangle \sim 1.7 \times 10^{-10}$ s (PEO) to $\langle\tau\rangle \sim 4.2 \times 10^{-10}$ s. Thus the mobility for amorphous PEO remains liquid-like even for the 10/90 composition, although the blend is 50 K below its DSC glass transition.[30] We believe that the weak changes in molecular motions may partly be explained by the present finding of an amorphous nanoheterogeneous structure, as previously discussed. The same structural scenario can, of course, partly explain the carbon relaxation behavior also for *a*-PMMA (Figure 6b). However, a full understanding of the component dynamics in solid PEO/PMMA blends will have to await temperature/frequency-dependent studies of relaxations.

Conclusions

We have presented a number of solid-state NMR experiments of PEO/*a*-PMMA over a wide concentration range. It is clear that separate amorphous (PEO/*a*-PMMA) and crystalline (pure PEO) phases are present for blends with PEO concentrations above ∼30% The degree of crystallinity has been quantified with ^{13}C equilibrium spectra. The analysis of lineshapes shows a gradually decreasing PEO crystallinity for increasing amounts of *a*-PMMA, consistent with DSC data[37] and with the behavior of the NMR relaxation decays ($T_{1\rho}$(H), $T_{1\rho}$(C), T_1(H), and T_1(C)) as the blend composition is varied.

From the observed influence of intermolecular spin diffusion on proton relaxations we conclude that the amorphous blends are homogeneous down to a length scale of at least ∼50 nm. Below this limit heterogeneities with average sizes larger than ∼2 nm exist, as indicated by the incompletely averaged proton $T_{1\rho}$(H) relaxations. Amorphous nanoheterogeneities appear also in the semicrystalline blends but cannot simply from the present data be related to specific regions with unique mobilities or spectral features.

The local mobility of amorphous PEO decreases in proportion to the amount of PMMA added to the blends, as revealed by the continuously changing carbon $T_{1\rho}$(C) and T_1(C). However, the relaxation behavior for PEO corresponds to relatively small changes in the average correlation time of motion and are estimated to be within an order of magnitude at most. The carbon relaxation times for *a*-PMMA are even less sensitive to blend composition, which may partly be due to α-CH_3-dominated relaxations.

Acknowledgment. This work was carried out with the support of the Swedish Research Council for Engineering Sciences. The author is grateful to Prof. Frans Maurer for helpful discussions and to Camilla Wästlund and Dr. Cynthia Khoo for providing the samples.

References and Notes

(1) Utracki, L. A. *Polymer Alloys and Blends*; Hanser Publishers: Munich, Vienna, New York, 1989.
(2) Martuscelli, E.; Silvestre, C.; Addonizio, M. L.; Amelino, L. *Makromol. Chem.* **1986**, *187*, 1557.
(3) Zawada, J. A.; Ylitalo, C. M.; Fuller, G. G.; Colby, R. H.; Long, T. E. *Macromolecules* **1992**, *25*, 2896.
(4) Liberman, S. A.; Gomes, A. S.; Macchi, E. M. *J. Polym. Sci., Polym. Chem. Ed.* **1987**, *22*, 2809.
(5) Brosseau, C.; Guillermo, A.; Cohen-Addad, J. P. *Polymer* **1992**, *33*, 2076.
(6) Brosseau, C.; Guillermo, A.; Cohen-Addad, J. P. *Macromolecules* **1992**, *25*, 4535.
(7) Martuscelli, E.; Demma, G.; Rossi, E.; Segre, A. L. *Polym. Commun.* **1983**, *24*, 266.
(8) Marco, C.; Fatou, J. G.; Gomez, M. A.; Tanaka, H.; Tonelli, A. E. *Macromolecules* **1990**, *23*, 2183.
(9) Wu, S. *J. Polym. Sci., Polym. Phys. Ed.* **1987**, *25*, 2511.
(10) Colby, R. H. *Polymer* **1989**, *30*, 1275.
(11) Ito, H.; Russell, T. P.; Wignall, G. D. *Macromolecules* **1987**, *20*, 2213.
(12) Hopkinson, I.; Kiff, F. T.; Richards, R. W.; King, S. M.; Farren, T. *Polymer* **1995**, *36*, 3523.
(13) Cortazar, M. M.; Calahorra, M. E.; Guzmán, G. M. *Eur. Polym. J.* **1982**, *18*, 165.
(14) Privalko, V. P.; Petrenko, K. D.; Lipatov, Yu. S. *Polymer* **1990**, *31*, 1277.
(15) Pedemonte, E.; Polleri, V.; Turturro, A.; Cimmino, S.; Silvestre, C.; Martuscelli, E. *Polymer* **1994**, *35*, 3278.
(16) Cimmino, S.; Martuscelli, E.; Silvestre, C. *Polymer* **1989**, *30*, 393.
(17) Li, X.; Hsu, S. L. *J. Polym. Sci., Polym. Phys. Ed.* **1984**, *22*, 1331.
(18) Alfonso, G. C.; Russell, T. P. *Macromolecules* **1986**, *19*, 1143.
(19) Addonizio, M. L.; Martuscelli, E.; Silvestre, C. *Polymer* **1987**, *28*, 183.
(20) John, E.; Jeon, S. H.; Ree, T. *J. Polym. Sci., Polym. Lett. Ed.* **1989**, *27*, 9.
(21) Martuscelli, E.; Canetti, M.; Vicini, C.; Seves, A. *Polym. Commun.* **1982**, *23*, 331.
(22) Silvestre, C.; Cimmino, S.; Martuscelli, E.; Karasz, F. E.; MacKnight, W. J. *Polymer* **1987**, *28*, 1190.
(23) Russell, T. P.; Ito, H.; Wignall, G. D. *Macromolecules* **1988**, *21*, 1703.

(24) Schantz, S. *Polym. Mater. Sci. Eng.* **1994**, *71*, 209.
(25) Straka, J.; Schmidt, P.; Dybal, J.; Schneider, B.; Spěvácek, J. *Polymer* **1995**, *36*, 1147.
(26) Schaefer, J.; Stejskal, E. O.; Buchdal, R. *Macromolecules* **1977**, *10*, 384.
(27) Stejskal, E. O.; Schaefer, J.; Sefcik, M. D.; McKay, R. A. *Macromolecules* **1981**, *14*, 275.
(28) Voelkel, R. *Angew. Chem., Int. Ed. Engl.* **1988**, *27*, 1468.
(29) McBrierty, V. J.; Packer, K. J. *Nuclear Magnetic Resonance in Solid Polymers*; Cambridge University Press: Cambridge, 1993.
(30) Khoo, C.; Wästlund, C.; Maurer, F. H. J. To be published.
(31) Sullivan, M. J.; Maciel, G. E. *Anal. Chem.* **1982**, *54*, 1615.
(32) Torchia, D. A. *J. Magn. Reson.* **1978**, *30*, 613.
(33) VanderHart, D. L.; Earl, W. L.; Garroway, A. N. *J. Magn. Reson.* **1981**, *44*, 361.
(34) Dechter, J. J. *J. Polym. Sci., Polym. Lett. Ed.* **1985**, *23*, 261.
(35) Johansson, A.; Tegenfeldt, J. *Macromolecules* **1992**, *25*, 4712.
(36) Miyazawa, T.; Fukushima, K.; Ideguchi, I. *J. Chem. Phys.* **1962**, *37*, 2764.
(37) Wästlund, C.; Maurer, F. H. J. To be published.
(38) Schantz, S.; Maunu, S. L. *Macromolecules* **1994**, *27*, 6915.
(39) Abragam, A. *The Principles of Nuclear Magnetic Magnetism*; Oxford University Press: Oxford, 1961.
(40) Packer, K. J.; Pope, J. M.; Yeung, R. R.; Cudby, M. E. A. *J. Polym. Sci., Polym. Phys. Ed.* **1984**, *22*, 589.
(41) Schantz, S.; Veeman, W. S. Manuscript in preparation.
(42) McBrierty, V. J.; Douglass, D. C. *J. Polym. Sci., Macromol. Rev.* **1981**, *16*, 295.
(43) Demco, D. E.; Johansson, A.; Tegenfeldt, J. *Solid State Nucl. Magn. Reson.* **1995**, *4*, 13.
(44) Clauss, J.; Schmidt-Rohr, K.; Spiess, H. W. *Acta Polym.* **1993**, *44*, 1.
(45) Rao, G. R.; Castiglioni, C.; Gussoni, M.; Zerbi, G.; Martuscelli, E. *Polymer* **1985**, *26*, 811.
(46) Marcos, J. I.; Orlandi, E.; Zerbi, G. *Polymer* **1990**, *31*, 1899.
(47) Dekmezian, A.; Axelson, D. E.; Dechter, J. J.; Borah, B.; Mandelkern, L. *J. Polym. Sci., Polym. Phys. Ed.* **1985**, *23*, 367.
(48) The carbon relaxations for *a*-PMMA showed nonexponential decays similar to the findings reported in refs 49 and 50. $T_{1\rho}$-(C) and T_1(C) in Figure 6b of the present study correspond to averages taken as the initial part of the respective relaxation decay.
(49) Fleming, W. W.; Lyerla, J. R.; Yannoni, C. S. In *NMR and Macromolecules*; ACS Symposium Series 247; Randall, J. C., Ed.; American Chemical Society: Washington, DC, 1984; Chapter 6, p 83.
(50) Edzes, H. T.; Veeman, W. S. *Polym. Bull.* **1981**, *5*, 255.

MA961538L